

# Simultaneous Computation with Multiple Prioritizations in Multi-Agent Motion Planning

Patrick Scheffe \*    Julius Kahle \*    Bassam Alrifae †

## Abstract

Multi-agent path finding (MAPF) in large networks is computationally challenging. An approach for MAPF is prioritized planning (PP), in which agents plan sequentially according to their priority. Albeit a computationally efficient approach for MAPF, the solution quality strongly depends on the prioritization. Most prioritizations rely either on heuristics, which do not generalize well, or iterate to find adequate priorities, which costs computational effort. In this work, we show how agents can compute with multiple prioritizations simultaneously. Our approach is general as it does not rely on domain-specific knowledge. The context of this work is multi-agent motion planning (MAMP) with a receding horizon subject to computation time constraints. MAMP considers the system dynamics in more detail compared to MAPF. In numerical experiments on MAMP, we demonstrate that our approach to prioritization comes close to optimal prioritization and outperforms state-of-the-art methods with only a minor increase in computation time. We show real-time capability in an experiment on a road network with ten vehicles in our Cyber-Physical Mobility Lab.

## Supplementary Materials

**Code** [github.com/embedded-software-laboratory/p-dmpc](https://github.com/embedded-software-laboratory/p-dmpc)

**Video** [youtu.be/Mb59zQ3j3s0](https://youtu.be/Mb59zQ3j3s0)

## 1 Introduction

### 1.1 Motivation

When solving multi-agent planning problems, agents may share objectives or be constrained by each other. Traditional multi-agent path finding (MAPF) is a multi-agent planning problem in which agents move in an environment represented by a graph  $\mathcal{G}_M = (\mathcal{V}_M, \mathcal{E}_M)$ , consisting of a set of vertices  $\mathcal{V}_M$ , which are locations, and a set of edges  $\mathcal{E}_M$ , which are paths between locations. The objective for each agent  $i$  is to move quickly from a start vertex  $s_i \in \mathcal{V}_M$  to a target vertex  $t_i \in \mathcal{V}_M$ . The constraints for each agent are to avoid collisions

---

\*Chair of Embedded Software, RWTH Aachen University, Im Süsterfeld 9, 52072 Aachen, Germany

†Department of Aerospace Engineering, University of the Bundeswehr Munich, Werner-Heisenberg-Weg 39, 85579 Neubiberg, Germany

with other agents. A collision occurs when two agents  $i$  and  $j$  at a time  $k$  are located at the same vertex  $v$ , represented by a tuple  $\langle i, j, v, k \rangle$ , or when they traverse the same edge  $(v - u) \in \mathcal{E}_M$ , represented by a tuple  $\langle i, j, v, u, k \rangle$ .

Solving a MAPF problem optimally is NP-hard (Yu, 2016; Yu & LaValle, 2013). Centralized approaches exploit the problem structure or lazily explore the solution space to increase their computational efficiency (e.g., Barer, Sharon, Stern, & Felner, 2021; Guo & Yu, 2024; Li, Ruml, & Koenig, 2021; Pan, Wang, Bi, Zhang, & Yu, 2024; Sharon, Stern, Felner, & Sturtevant, 2015; Yu, 2020). Prioritized planning (PP), introduced by Erdmann and Lozano-Pérez (1987), is a computationally more efficient method for MAPF. Instead of solving a MAPF problem optimally, PP divides the problem into multiple subproblems, and each agent solves only its subproblem. Since the subproblems are smaller in size compared to the centralized problem, the computation time is reduced. Additionally, agents can compute the solution in a distributed fashion.

While efficient, PP often produces suboptimal solutions and is not guaranteed to find a solution at all. In the example in Figure 1, out of the six possible prioritizations, only the two in which agent 2 has the lowest priority produce a solution. This is referred to as the incompleteness of PP: while some prioritizations can result in solutions, others may not (Ma, Harabor, Stuckey, Li, & Koenig, 2019). Given an underlying planning method, the prioritization determines the cost of the solution.

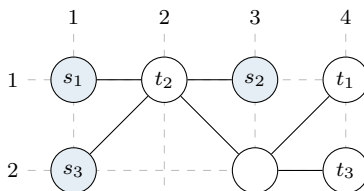


Figure 1: A MAPF instance in which PP results in a solution only if agent 2 has lowest priority. Example adjusted from Ma et al. (2019).

If we view prioritization and planning as a two-stage optimization, the solution given a prioritization can be seen as a local optimum. In general, for  $N_A$  agents, there exist up to  $N_A!$  prioritizations. Let  $J_p$  denote the networked cost given a prioritization  $p$ . In traditional MAPF, the networked cost is measured in terms of the flowtime, i.e., the sum of travel times of all agents, or the makespan, i.e., the maximum travel time of all agents.

**Definition 1.** The optimal prioritization  $p^*$  is defined as the prioritization which yields the optimal solution in terms of the networked cost,

$$p^* = \arg \min_p J_p. \quad (1)$$

The solution given the optimal prioritization is denoted as the global optimum in PP, which notably can be different from the optimal solution to the multi-agent planning problem. A core challenge in PP is finding a prioritization that results in a solution with a low networked cost.

To approach the global optimum, traditional approaches rely on heuristics to reduce the networked cost (e.g., Chen et al., 2023; Kloock, Scheffe, Marquardt, et al., 2019; Scheffe,

Dorndorf, & Alrifae, 2022; Wu, Bhattacharya, & Prorok, 2020; Yao & Zhang, 2018). Such heuristic approaches require domain-specific knowledge, making them unsuitable for generalized application. Further, their performance can be subpar, as heuristics are often tailored towards specific planning problems.

In domain-independent approaches, there is usually no a-priori knowledge about which prioritization yields a close-to-optimal solution. Thus, the prioritization must be optimized, which involves computing multiple solutions using different prioritizations. However, computing multiple solutions sequentially might be intractable for real-time applications with constrained computation time. Consequently, a simultaneous computation of multiple solutions is needed.

## 1.2 Related Work

Figure 2 displays the computations of three interacting, sequentially computing agents. The width of a block represents the computation time of each computation.

When selecting the prioritization, heuristics are often consulted. Heuristics aim to improve the prioritization mostly for their domain-dependent objective, and are thus less likely to generalize well. The following approaches use objective-based heuristics for prioritization to improve the networked cost. As illustrated in Figure 2a, these approaches solve PP problem using a single prioritization. We first present traditional MAPF approaches (van den Berg & Overmars, 2005; Wu et al., 2020; Zhang, Li, Huang, & Koenig, 2022). In (Wu et al., 2020), the prioritization is determined by the number of possible paths a robot can take to reach its goal. The lower this number is, the higher is a robot’s priority. Thereby, the probability for each robot to find a solution is meant to be increased, which directly affects the networked cost. In (van den Berg & Overmars, 2005), robots with longer estimated travel distances receive higher priority to more evenly distribute the travel time among robots. Zhang et al. (2022) proposes a prioritization algorithm based on machine learning, which performs competitively compared to heuristic algorithms. Our previous work (Kloock, Scheffe, Marquardt, et al., 2019) prioritizes agents with the goal of increasing the traffic flow rate at a road intersection through a heuristic based on the remaining time before an agent enters the intersection. In (Yao & Zhang, 2018), automated vehicles approaching an intersection are prioritized using mixed integer programming. Both the prioritization and the vehicle’s speed are optimized to minimize the travel time of the vehicles. The algorithm in (Chalaki & Malikopoulos, 2022) prioritizes vehicles on intersections using job-shop scheduling and thereby reduces the vehicles’ average travel time.

Instead of finding a good prioritization heuristically, other works optimize the prioritization. As illustrated in Figure 2b, these approaches solve the networked planning problem by exploring multiple prioritizations sequentially. These approaches aim to improve the solution quality by investing computation time. Bennewitz, Burgard, and Thrun (2002) propose a randomized hill-climbing search for finding the optimal prioritization. Beginning at an initial prioritization, priorities of agents are swapped randomly to increase the solution quality. Recomputing the solution in each iteration increases the computation effort. Ma et al. (2019) present an algorithm to lazily explore the space of all possible prioritizations. Whenever a conflict between two agents occurs, both possible prioritizations are added to a

search tree. Thus, the computation effort depends on the number of needed iterations until a conflict-free prioritization is found.

Sequential computation regarding a prioritization yields periods of idle time in each agent. The problem of reducing idle time due to sequential operation is addressed in production automation. Johnson’s rule (Almhanna, Al-Turaihi, & Murshedi, 2023) and sequencing (Mak, Rong, & Zhang, 2014) are methods to decrease idle time by optimizing the assignment and sequence for jobs on machines in assembly lines. Further, Çam and Sezen (2020) reduce idle time of control systems, i.e., unproductive time of the system, but not idle time during computation.

Our strategy for reducing idle time in sequential computation is to parallelize computation. For parallel computation, agents can be distributed physically, with several processing units on several agents, or logically, with several processing units on a central entity. Parallel computation usually deteriorates the solution quality. In our previous work (Scheffe, Xu, & Alrifae, 2024), overapproximating constraints results in a potentially more conservative solution. Conflict-driven approaches (e.g., Čáp, Novák, Kleiner, & Selecký, 2015; Ma et al., 2019; Sharon et al., 2015), start with parallel computation but require recomputation whenever a conflict arises.



(a) Solving the PP problem with a single prioritization (e.g., Chalaki & Malikopoulos, 2022; Kloock, Scheffe, Marquardt, et al., 2019; van den Berg & Overmars, 2005; Wu et al., 2020; Yao & Zhang, 2018).



(b) Solving the PP problem with three prioritizations sequentially (e.g., Bennewitz et al., 2002; Ma et al., 2019). Note how the order of computation changes with the prioritization.



(c) Solving the PP problem with three prioritizations simultaneously (our approach). Note how rows represent the different prioritizations from Figure 2b, and each agent solves only one agent planning problem corresponding to a different prioritization at a time.

Figure 2: Exemplary illustration of the computation time in different prioritization approaches in an example with three agents represented in  $\mathcal{V}_1$ ,  $\mathcal{V}_2$ , and  $\mathcal{V}_3$ ; blocks indicate computation time of agents.

### 1.3 Contribution

In PP, the optimality of the solution depends on the prioritization. To find the optimal prioritization and therefore the global optimum of the PP problem, the set of possible prioritizations and their corresponding solutions to the PP problem needs to be explored. If computation time is limited, such as in real-time applications, the sequential computation of multiple solutions can be intractable. This paper presents an approach that exploits the sequential nature of PP to explore multiple prioritizations simultaneously. Our approach improves the solution quality over sequential computation with a single prioritization while keeping computation time short. We select prioritizations such that (i) we always improve or maintain the solution quality of a previously found prioritization, and (ii) all explored prioritizations are computed simultaneously. The latter requires establishing a Latin square, the general form of a Sudoku puzzle.

We illustrate the benefit of our approach in an example with three interacting, sequentially computing agents in Figure 2. A block shows the computation time of an agent. Figure 2a shows how approaches based on heuristics solve the PP problem for only a single prioritization. The solution quality strongly depends on the heuristic. Figure 2b shows how the PP problem can be solved multiple times sequentially regarding multiple prioritizations. Even though it can improve solution quality, it prolongs the computation time. In this work, we make use of the fact that in sequential computation the agents idle most of the time: In the example shown in Figure 2a, agents idle two-thirds of the available time. Figure 2c showcases our approach: By utilizing the idle time, we solve the PP problem regarding the three prioritizations from Figure 2b simultaneously.

Applying our strategy to the example in Figure 1, we always explore a prioritization in which agent 2 has the lowest priority.

### 1.4 Structure of this Article

The rest of this article is organized as follows. In Section 2, we formalize time-variant coupling and prioritization of agents in a receding horizon planning framework. In Section 3, we formulate requirements for simultaneously computable prioritizations. We further present our algorithm for simultaneous computation, which can both retain prioritizations to utilize the predictive nature of receding horizon planning, and explore new prioritizations to increase the likelihood of finding a solution. In particular, the time required for exploration spreads across consecutive time steps, which keeps computation time at each time step short. A variant of MAPF is multi-agent motion planning (MAMP), in which the kinodynamic constraints of agents are taken into account during planning. We present our multi-agent motion planner for connected and automated vehicles (CAVs) driving on roads in Section 4. In Section 5, we present a comparison of our approach to state-of-the-art prioritization approaches in numerical experiments with CAVs, and showcase real-time capabilities of our approach in an experiment with ten CAVs in our Cyber-Physical Mobility Lab (CPM Lab).

## 2 Preliminaries

This section provides the background to prioritized receding horizon planning. In PP, agents first receive all predictions from their predecessors, then solve the planning problem, and finally send their predictions to their successors. To determine the predecessors and successors of agents, we couple and prioritize them. The following section introduces our notation and the background on coupling, prioritization, and receding horizon planning.

### 2.1 Notation

In this paper, we refer to agents whenever concepts are generally applicable to PP. We assume that states of agents are observable, and therefore we refer to states instead of outputs. The definitions and methods can be transferred to outputs as well, which we omit for brevity. We denote scalars with normal font, vectors with bold lowercase letters, matrices with bold uppercase letters, and sets with calligraphic uppercase letters. For any set  $\mathcal{S}$ , the cardinality of the set is denoted by  $|\mathcal{S}|$ . A variable  $x$  is marked with a superscript  $x^{(i)}$  if it belongs to agent  $i$ . The actual value of a variable  $x$  at time  $k$  is written as  $x(k)$ , while values predicted for time  $k+l$  at time  $k$  are written as  $x_{k+l|k}$ . A trajectory is denoted by replacing the time argument with  $(\cdot)$  as in  $x_{\cdot|k}$ .

We use graphs as a modeling tool of networked control system (NCS). Every agent is associated with a vertex, so the terms are used synonymously.

**Definition 2** (Undirected graph). An undirected graph  $\mathcal{G} = (\mathcal{V}, \mathcal{E})$  is a pair of two sets, the set of vertices  $\mathcal{V} = \{1, \dots, N_A\}$  and the set of undirected edges  $\mathcal{E} \subseteq \mathcal{V} \times \mathcal{V}$ . The edge between  $i$  and  $j$  is denoted by  $(i - j)$ .

**Definition 3** (Directed graph). A directed graph  $\vec{\mathcal{G}} = (\mathcal{V}, \vec{\mathcal{E}})$  is a pair of two sets, the set of vertices  $\mathcal{V} = \{1, \dots, N_A\}$  and the set of directed edges  $\vec{\mathcal{E}} \subseteq \mathcal{V} \times \mathcal{V}$ . The edge from  $i$  to  $j$  is denoted by  $(i \rightarrow j)$ . An oriented graph is a directed graph obtained from an undirected graph by replacing each edge  $(i - j)$  with either  $(i \rightarrow j)$  or  $(j \rightarrow i)$ .

### 2.2 Coupling

If agents interact via their objectives or constraints, we speak of coupled agents. A coupling graph represents the interaction between agents.

**Definition 4** (Undirected coupling graph). An undirected coupling graph  $\mathcal{G}(k) = (\mathcal{V}, \mathcal{E}(k))$  is a graph that represents the interaction between agents at time step  $k$ . Vertices  $i \in \mathcal{V} = \{1, \dots, N_A\}$  represent agents, and edges  $(i - j) \in \mathcal{E}$  represent coupling objectives and constraints between agents.

The application in which PP is used determines which coupling objectives and constraints must be considered in an agent’s planning problem. For example, in MAPF, coupling constraints are introduced to achieve collision avoidance.

The undirected coupling graph can often be determined before planning starts. For example, in robot applications with a fixed time horizon, the robots’ movement range in this time horizon can be used to determine couplings (Scheffe, Xu, & Alrifae, 2024). Alternatively, if robots follow fixed paths, the paths’ intersections determine couplings between

robots. This can be the case for road vehicles following lanes, or for warehouse robots (Li, Hoang, Lin, Vu, & Koenig, 2023; Ma, Li, Kumar, & Koenig, 2017). If no prior knowledge on the coupling is available, but the coupling is critical, all agents must be connected.

### 2.3 Prioritization

In PP, we prioritize agents, which results in clear responsibilities considering coupling objectives and constraints during planning (Alrifae, Heßeler, & Abel, 2016; Kuwata, Richards, Schouwenaars, & How, 2007). A fixed or time-invariant prioritization function  $p: \mathcal{V} \rightarrow \mathbb{N}$  prioritizes every agent. If  $p(i) < p(j)$ , then agent  $i$  has a higher priority than agent  $j$ .

By prioritizing, we can orient the edges of an undirected coupling graph to form a directed coupling graph.

**Definition 5** (Directed coupling graph). A directed coupling graph  $\vec{\mathcal{G}}(k) = (\mathcal{V}, \vec{\mathcal{E}}(k))$  is an oriented graph obtained from orienting the edges of an undirected coupling graph at time step  $k$ . If an edge  $(i \rightarrow j)$  is directed from agent  $i$  to agent  $j$ , then agent  $j$  is responsible for considering the respective coupling objective and constraint in its planning problem.

An edge points towards the vertex with lower priority,

$$(i \rightarrow j) \in \vec{\mathcal{E}} \iff p(i) < p(j) \wedge (i - j) \in \mathcal{E}. \quad (2)$$

The prioritization function thus constitutes a strict partial order  $<$  on the agent set  $\mathcal{V}$ ,

$$i < j \iff p(i) < p(j). \quad (3)$$

The order is partial, as opposed to total, since a relation exists only for coupled agents. For the strict partial order—and thus the orientation of every edge—to be well-defined, a valid prioritization function needs to assign pairwise different priorities to vertices that are connected by an edge:

$$p(i) \neq p(j), \quad \forall i, j \in \mathcal{V}, \forall (i - j) \in \mathcal{E}, i \neq j. \quad (4)$$

Given the construction rule in (2), the directed coupling graph  $\vec{\mathcal{G}}$  resulting from the undirected coupling graph  $\mathcal{G}$  and a valid prioritization function  $p$  regarding (4) is a directed acyclic graph (DAG) (Scheffe, Kahle, & Alrifae, 2023).

Since in PP, an agent requires its predecessors’ plans to consider coupling objectives and constraints, the agents must solve their planning problems in a sequential order. This order, as well as the communication links, are deducible from the directed coupling graph by traversing the graph along its edges.

### 2.4 Receding Horizon Planning

A strategy to further reduce computation time in PP is by introducing a fixed time horizon. Instead of solving the MAPF problem from start to end, only a certain number of time steps is considered. The problem is solved repeatedly over the course of time, a practice known as receding horizon planning or online replanning (Li, Tinka, et al., 2021; Scheffe, Pedrosa,

Flaßkamp, & Alrifae, 2023; Shahar et al., 2021; Silver, 2005). Agents apply actions until the next planning result is available.

In each time step of receding horizon planning, priorities can be reassigned, which results in a time-variant prioritization. We redefine the time-invariant prioritization function to a time-variant prioritization function. It is a function  $p: \mathcal{V} \times \mathbb{N} \rightarrow \mathbb{N}$  which prioritizes each agent  $i$  at each time step  $k$ . We indicate a time-invariant prioritization by replacing the time argument with a dash, as in  $p(i, -)$ . In our approach, the priority ordering is consistent during planning for the planning horizon, but can change whenever agents plan.

In accordance with the usage in the literature (e.g., Ma et al., 2019; Wu et al., 2020), we define completeness as follows.

**Definition 6** (Completeness). A prioritized planning method is complete if given an underlying planning method, any prioritization results in a solution for every MAPF instance.

We extend the considerations in (Ma et al., 2019) from fixed prioritizations to time-variant prioritizations.

**Theorem 1.** *In general, prioritized planning with time-variant prioritization is incomplete.*

*Proof.* A counterexample is given in Figure 3. This example requires the highest-priority agent to take a suboptimal action with regards to its own objective in order to create a solution to the MAPF problem. The highest-priority agent, however, always takes an optimal action in prioritized planning.  $\square$

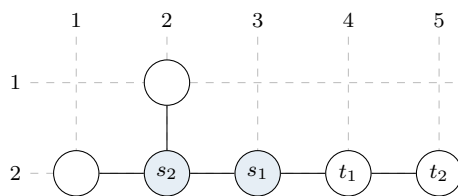


Figure 3: A MAPF instance which is not TP-solvable.

**Definition 7** (P-solvable, according to (Ma et al., 2019)). A MAPF instance is P-solvable iff there exists a solution for some fixed prioritization  $p(i, -)$ .

**Definition 8** (TP-solvable). A MAPF instance is TP-solvable iff there exists a solution for some time-variant prioritization  $p(i, k)$ .

**Theorem 2.** *The class of TP-solvable MAPF instances includes the class of P-solvable MAPF instances.*

*Proof.* A time-variant prioritization can mimic a fixed prioritization by using the same ordering at every time step,

$$p(i, k) := p(i, -). \quad (5)$$

Therefore, every MAPF instance that is solvable with a fixed prioritization is solvable with a time-variant prioritization.  $\square$



**Theorem 3.** *Prioritized planning with a time-variant prioritization is incomplete for the class of TP-solvable MAPF instances.*

*Proof.* For the MAPF instance displayed in Figure 4, a time-variant prioritization that does not result in a solution is any fixed prioritization.  $\square$

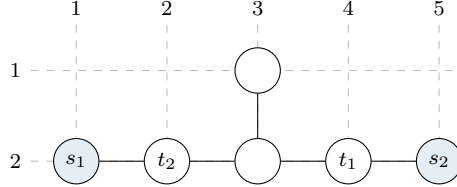


Figure 4: A MAPF instance which is not P-solvable (Ma et al., 2019), but is TP-solvable with a priority flip in the third time step. Figure redrawn from Ma et al. (2019).

### 3 Exploring Multiple Prioritizations Simultaneously

This section presents the core idea of this paper, which is to improve the solution quality of a given prioritization by exploring multiple other prioritizations simultaneously. We state the requirements for prioritizations with which simultaneous computation is possible in Section 3.1. Building on these requirements, we present the algorithm for selecting a set of prioritizations and simultaneously computing with these prioritizations in Section 3.2. In Section 3.3, we show theoretically that our approach can both retain prioritizations to utilize the predictive nature of receding horizon planning and explore new prioritizations to increase the likelihood of finding a solution.

#### 3.1 Parallelizable Prioritizations

In this section, we establish the requirements for prioritizations with which simultaneous computation is possible. Our goal of improving the solution quality compared to a given prioritization implies the assumption that an initial valid prioritization according to (4) is given. Finding an initial valid prioritization is simple, e.g., a prioritization that assigns priorities according to unique vertex numbers is valid. Other prioritization algorithms exist (Kuwata et al., 2007; Scheffe et al., 2022; Scheffe, Kahle, & Alrifaae, 2023).

The computation order of agents in PP can be structured with agent classes  $\mathfrak{V}$ . Agents belonging to the same agent class can solve their planning problem in parallel. An undirected coupling graph  $\mathcal{G} = (\mathcal{V}, \mathcal{E})$  and a prioritization function  $p$  form a directed coupling graph  $\vec{\mathcal{G}}$  with (2). By topologically sorting the directed coupling graph, we map agents to classes  $\mathfrak{V}$  according to our Algorithm 1. The algorithm inspects all vertices to find sources, i.e., vertices with no incoming edges (Line 6). All sources can start their computation, so we add them to a class (Line 7). The resulting class is next in solving its planning problem, so it is added to the computation sequence (Line 10). The processed vertices are removed from the set of vertices to process (Line 11). Finally, all edges connected to the processed vertices are removed from the coupling graph (Lines 12 to 14). The loop repeats until all vertices are

---

**Algorithm 1** Find agent classes, adapted from Alrifaae et al. (2016)

---

**Input:** Directed coupling graph  $\vec{\mathcal{G}} = (\mathcal{V}, \vec{\mathcal{E}})$

**Output:** Agent classes in sequence  $(s_z)_{z=1}^{N_c}$

```

1:  $N_c \leftarrow 0$  ▷ number of classes
2:  $\mathcal{V}_{\text{todo}} \leftarrow \mathcal{V}$  ▷ remaining agents
3: while  $\mathcal{V}_{\text{todo}} \neq \emptyset$  do
4:    $N_c \leftarrow N_c + 1$ 
5:   for  $i \in \mathcal{V}_{\text{todo}}$  do
6:     if  $d^{(i \leftarrow)} = 0$  then
7:        $\mathcal{V}_{N_c} \leftarrow \mathcal{V}_{N_c} \cup i$  ▷ sources can compute
8:     if  $\mathcal{V}_{N_c} = \emptyset$  then
9:       return FAILURE ▷ Graph is no DAG
10:     $s_{N_c} \leftarrow \mathcal{V}_{N_c}$ 
11:     $\mathcal{V}_{\text{todo}} \leftarrow \mathcal{V}_{\text{todo}} \setminus \mathcal{V}_{N_c}$ 
12:    for  $i \in \mathcal{V}_{N_c}$  do
13:      for  $j \in \mathcal{V}_{\text{todo}}$  do
14:         $\vec{\mathcal{E}} \leftarrow \vec{\mathcal{E}} \setminus (i \rightarrow j)$ 
15: return  $(s_z)_{z=1}^{N_c}$ 

```

---

assigned to classes. The output of Algorithm 1 is a sequence of agent classes  $(s_z)_{z=1}^{N_c}$  which orders the agent classes  $\mathfrak{V} = \{\mathcal{V}_1, \dots, \mathcal{V}_{N_c}\}$ . This computation sequence represents the order in which the agent classes can solve their planning problems.

**Definition 9** (Computation sequence). The set of agent classes  $\mathfrak{V}$  is a countable set with  $|\mathfrak{V}| = N_c$ . The computation sequence defined as

$$(s_z)_{z=1}^{N_c} = (s_1, s_2, \dots, s_{N_c}) \quad (6)$$

with the domain  $\{1, \dots, N_c\}$  and the codomain  $\mathfrak{V}$  resembles a permutation of the agent classes in  $\mathfrak{V}$ .

Figure 5 shows an example of Algorithm 1 for a directed coupling graph with four agents. The resulting computation sequence is  $(\{1\}, \{2, 3\}, \{4\})$ .

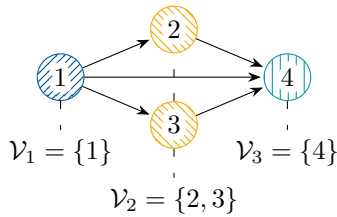


Figure 5: Example coupling graph for Algorithm 1, and resulting agent classes in sequence.

Algorithm 1 returns a computation sequence with the minimum number of sequential computations for the given directed coupling graph. We can also invert this process, i.e., we

can generate a valid prioritization corresponding to a computation sequence. W.l.o.g., for two classes  $\mathcal{V}_1, \mathcal{V}_2 \in \mathfrak{V}$ ,  $\mathcal{V}_1 \neq \mathcal{V}_2$ , and with  $i \in \mathcal{V}_1$  and  $j \in \mathcal{V}_2$  it must hold that

$$p(i) \neq p(j). \quad (7)$$

According to (4), agents in the same class may have equal priorities as they are not connected by an edge. However, since we allow time-variant coupling graphs, we enforce unique priorities among agents (cf. Section 3.3). A valid prioritization corresponding to the computation sequence is given by

$$p(i) = Z \cdot N_A + i, \quad i \in s_Z \in (s_z)_{z=1}^{N_c}, \quad (8)$$

with an agent  $i$ , and the sequence index  $Z$ . For the example in Figure 5, this function would yield

$$p(1) = 5, \quad p(2) = 10, \quad p(3) = 11, \quad p(4) = 16. \quad (9)$$

The problem of finding the optimal permutation of agent classes can formally be stated as follows.

**Problem 1.** Given a set of agent classes  $\mathfrak{V}$ , find a computation sequence  $(s_z)_{z=1}^{N_c}$  resulting in a prioritization function  $p_q$  with (8) that minimizes the sum of the costs of all agents

$$p_q = \arg \min_p J_p. \quad (10)$$

Note that finding the optimal sequence does not necessarily coincide with finding the optimal prioritization, as the permutations of sequences may not express the permutations of prioritizations.

Problem 1 is known as the Drilling Problem, which is a problem in combinatorial optimization (Korte & Vygen, 2018, p.1). Given a set of holes that need to be drilled, the Drilling Problem consists of finding a permutation of the order in which they need to be drilled to minimize the total distance the drill needs to travel. As the set of classes contains  $|\mathfrak{V}| = N_c$  elements, for Problem 1, this would result in  $|\mathcal{S}| = N_c!$  different permutations. A possible solution to that problem is enumerating all  $N_c!$  sequences (Azarm & Schmidt, 1997; Korte & Vygen, 2018): Given a set  $\mathfrak{V}$  of  $N_c$  classes, solve PP problems regarding each of the  $N_c!$  sequences and choose the one with minimal cost. However, the computation time of this approach increases rapidly with the number of classes.

As solving Problem 1 is computationally intractable with real-time constraints, we aim to solve the following problem.

**Problem 2.** Given a set of agent classes  $\mathfrak{V}$ , find  $N_c = |\mathfrak{V}|$  different computation sequences such that all sequences can be computed simultaneously.

Our goal in Problem 2 is to find  $N_c$  sequences out of  $N_c!$  that can be computed simultaneously. A class  $\mathcal{V}_l \in \mathfrak{V}$  can solve exactly one planning problem regarding a specific computation sequence in each time slot. To formalize the task, we introduce a computation schedule matrix  $\mathbf{S} \in \mathfrak{V}^{N_c \times N_c}$  which contains  $N_c$  computation sequences as rows. Each column of  $\mathbf{S}$  represents a time slot in the networked computation. The matrix  $\mathbf{S}$  represents a valid computation schedule if its entries fulfill

$$s_{ij} \neq s_{ik}, \quad i, j, k \in \{1, \dots, N_c\}, j \neq k, \text{ and} \quad (11)$$

$$s_{ij} \neq s_{kj}, \quad i, j, k \in \{1, \dots, N_c\}, i \neq k. \quad (12)$$

We ensure valid computation sequences with (11), and we ensure that each class solves exactly one planning problem in each time slot with (12). The matrix resulting from these conditions is also known as a Latin square. Adapted from McKay and Wanless (2005), a Latin square  $\mathbf{L} \in \{1, \dots, N\}^{N \times N}$  is a matrix in which each row and column contains only distinct entries. That is, each row and column contains every element in  $\{1, \dots, N\}$  exactly once. For  $\mathbf{S}$ , the property of distinct entries in each row and column is given by (11) and (12), respectively. The problem is related to a Sudoku puzzle: The solution to a Sudoku puzzle is a Latin square with  $N = 9$  with the additional rule that each of the nine non-overlapping  $3 \times 3$  partial matrices contain every element in  $\{1, \dots, N\}$  exactly once.

### 3.2 Simultaneous Computation with Multiple Prioritizations

This section describes our algorithms for simultaneous computation with multiple prioritizations. We first present our decentralized algorithm through which every agent obtains the same computation schedule matrix which fulfills (11) and (12). We then show how agents solve PP problems with multiple prioritizations. Finally, we show how agents select a solution for the PP problems.

Our goal for the computation schedule matrix  $\mathbf{S}$  is to explore  $N_c$  prioritizations in a time step to increase the probability of finding the optimal prioritization according to Problem 1. Algorithm 2 is our decentralized algorithm to find a computation schedule matrix  $\mathbf{S}$ . We restate that a row  $\mathbf{s}_q \in 1 \times N_c$  corresponds to a computation sequence  $q$ , and a column  $\mathbf{s}_m \in N_c \times 1$  corresponds to a time slot  $m$  during the networked computation. First, we initialize the computation schedule matrix  $\mathbf{S}$  with the size  $N_c \times N_c$  and fill the first row  $\mathbf{s}_1$  with the classes of  $\mathfrak{V}$  in sequence (Lines 1 and 2). Note that this initial row can change from one time step to another as it depends on the initial prioritization. We enforce a common random seed among agents for consistent results of the algorithm (Line 4). The algorithm determines the remaining rows in a loop (Line 5). For each row, the algorithm loops over all  $N_c$  columns that need to be populated (Lines 7 and 8). We use the number of available classes in each column that can form a valid computation schedule matrix as a heuristic for the order in which the columns are populated (Line 10). This number of available classes is stored in the `options` array. It is an array of sets, each containing all elements of  $\mathfrak{V}$  that respect (11) regarding the current row  $q$  and that respect (12) regarding the column corresponding to the array index. The next column to populate is the one with the least number of available classes (Line 11). One of these classes is selected at random (Line 15). If all columns are populated with valid entries, we progress to the next row (Line 18). If there is a column for which no classes are available to select from, the current row is invalid with the rest of the computation schedule matrix (Line 12), so we reset the current row (Line 20) and start over.

We illustrate Algorithm 2 with an example in Figure 6. The figure contains four agent classes, and depicts the construction of the second row of the computation schedule matrix. Each other row in the figure corresponds either to determining the remaining options of computation classes for each cell (Line 10), or to the random selection of an option (Line 15) from the most constrained cell (Line 11).

Our Algorithm 2 builds a computation schedule row by row, which is valid according to (11) and (12). A partly built, valid computation schedule can always be completed.

---

**Algorithm 2** Decentralized construction of computation schedule matrix  $\mathbf{S}$ 


---

**Input:** Set of agent classes  $\mathfrak{V}$

**Output:** Computation schedule matrix  $\mathbf{S}$

```

1:  $\mathbf{S} \leftarrow$  empty matrix of size  $N_c \times N_c$ 
2:  $\mathbf{s}_1. \leftarrow [\mathcal{V}_1, \mathcal{V}_2, \dots, \mathcal{V}_{N_c}]$ 
3:  $q \leftarrow 1$ 
4: initialize random seed with current time step  $\triangleright$  for consistency across agents
5: while  $q < N_c$  do  $\triangleright$  find remaining columns
6:   is_valid  $\leftarrow$  true
7:    $N_{\text{cols-todo}} \leftarrow N_c$ 
8:   while  $N_{\text{cols-todo}} > 0$  do
9:     for  $m = 1, \dots, N_c$  do
10:       $\text{options}[m] \leftarrow \mathfrak{V} \setminus (\mathbf{s}_q. \cup \mathbf{s}.m)$ 
11:       $m \leftarrow \arg \min_i |\text{options}[i]|$ 
12:      if  $|\text{options}[i]| = 0$  then
13:        is_valid  $\leftarrow$  false
14:        break
15:       $s_{qm} \leftarrow \text{RANDOM}(\text{options}[m])$ 
16:       $N_{\text{cols-todo}} \leftarrow N_{\text{cols-todo}} - 1$ 
17:   if is_valid then
18:      $q \leftarrow q + 1$ 
19:   else
20:      $\mathbf{s}_q. \leftarrow$  empty vector of size  $1 \times N_c$ 
21: return  $\mathbf{S}$ 

```

---

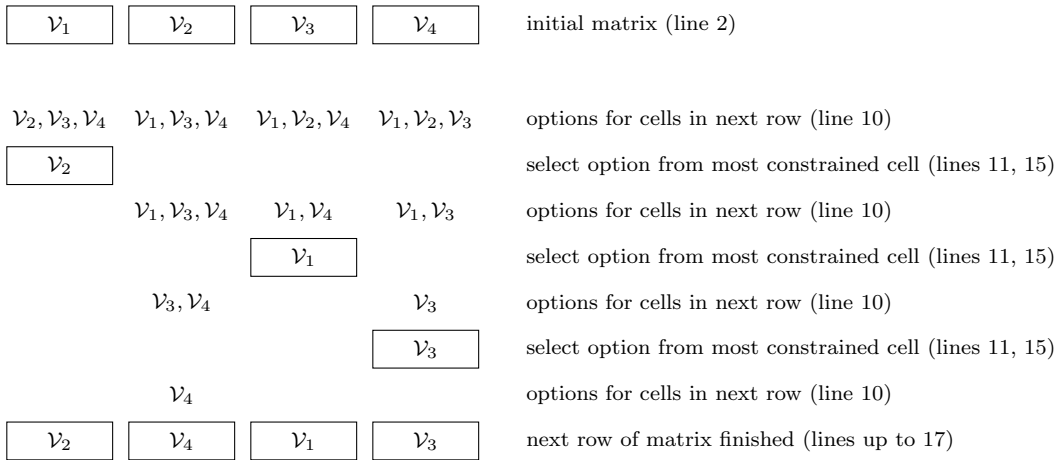


Figure 6: Example for Algorithm 2 which builds a computation schedule matrix.

Therefore, our Algorithm 2 will eventually converge to a valid computation schedule. Due to the randomness of the approach, there is no bound on the number of required iterations until convergence, which could be addressed with a more sophisticated algorithm. In practice, the computation time to build a computation schedule matrix is negligible when compared to the computation time for motion planning.

Computation with multiple prioritizations is similar in concept to computation with a single prioritization. The main difference is that there are  $N_c$  different directed coupling graphs  $\vec{\mathcal{G}}_{p_q} = (\mathcal{V}, \vec{\mathcal{E}}_{p_q})$ , and with it sets of predecessors  $\mathcal{V}_{p_q}^{(i\leftarrow)}$ , successors  $\mathcal{V}_{p_q}^{(i\rightarrow)}$ , and neighbors  $\mathcal{V}_{p_q}^{(i)}$ , defined as

$$\mathcal{V}_{p_q}^{(i\leftarrow)} = \{j \in \mathcal{V} \mid (j \rightarrow i) \in \vec{\mathcal{E}}_{p_q}\}, \quad (13)$$

$$\mathcal{V}_{p_q}^{(i\rightarrow)} = \{j \in \mathcal{V} \mid (i \rightarrow j) \in \vec{\mathcal{E}}_{p_q}\}, \quad (14)$$

$$\mathcal{V}_{p_q}^{(i)} = \mathcal{V}_{p_q}^{(i\leftarrow)} \cup \mathcal{V}_{p_q}^{(i\rightarrow)}. \quad (15)$$

Each agent performs  $N_c$  computations in  $N_c$  time slots. An agent in class  $\mathcal{V}_l$  finds the sequence  $\mathbf{s}_q$  corresponding to a time slot  $m$  by looking for its agent class in the respective column of the computation schedule matrix. For this computation sequence it must hold

$$s_{qm} = \mathcal{V}_l. \quad (16)$$

From this sequence, the agent constructs the directed coupling graph  $\vec{\mathcal{G}}_{p_q}$  with (2) and (8). The agent solves its planning problem after receiving the required information from its predecessors  $\mathcal{V}_{p_q}^{(i\leftarrow)}$ . It then stores the solution cost corresponding to the sequence  $q$  as an element in a solution cost array.

After all computation sequences are solved, each agent broadcasts its solution cost array. With this information, each agent can determine the solution quality of every computation sequence. We define the solution quality as the networked cost  $J(k)$  of a time step  $k$ . The networked cost for each computation sequence  $q$  is given as the sum of the costs of all agent planning problems regarding the corresponding computation sequence

$$J_{p_q}(k) = \sum_{i=1}^{N_A} J_{p_q}^{(i)}(k), \quad (17)$$

with the solution cost  $J_{p_q}^{(i)}: \mathbb{N} \rightarrow \mathbb{R}$  of an agent  $i$ , the sequence  $q$  corresponding to a prioritization function  $p_q$  with (8), and a time step  $k$ . After receiving the solution cost arrays of all other agents, each agent selects the computation sequence with the highest solution quality, i.e., the minimal networked cost.

### 3.3 Initial Prioritization

The selection of the initial prioritization, and with Algorithm 1 the initial computation sequence as well, determines which prioritizations can possibly be explored. We identified two objectives for selecting the initial prioritization.

The time-variance of priorities in receding horizon planning has both advantages and disadvantages. An advantage of time-variance is that situations which dictate varying priorities over time to find a solution can be solved, as illustrated by Figure 4. A disadvantage

is that the constraints in an agent’s planning problem change with the prioritization. This change in the constraints can counteract the predictive nature of a receding horizon planning algorithm, which can affect the solution quality (Scheffe, Kahle, & Alrifae, 2023). If changes in the planning problem are small, retaining priorities can be beneficial. One objective is to enable the algorithm to retain priorities. The other objective is to explore many priorities to find the best available solution. A poor selection of an initial set of agent classes can limit the exploration of prioritizations to a fraction of the number of possible prioritizations.

We achieve the first objective by using the computation sequence with the lowest cost according to (17) from a previous time step for the initial prioritization. From this computation sequence, we generate priorities with (8). To guarantee the validity of these priorities according to (4), they must be unique to account for the time-variability of the coupling graph. In the next time step, we orient the undirected coupling graph by prioritizing agents with the retained priorities, thus creating a directed coupling graph. From this directed coupling graph, we construct the initial computation sequence with our Algorithm 1. With this process, it is always possible to maintain the priorities of the previous time step even with a time-variant coupling graph.

We took a step towards the second objective by random construction of the computation schedule matrix in Algorithm 2. However, given a computation sequence, only a subset of computation schedule matrices can be constructed. The question remains: which computation sequences can be explored given an initial sequence? We explore different computation sequences if we build unique computation schedule matrices. Two computation schedule matrices are unique if the set of their rows are different, i.e., if one matrix contains a computation sequence that the other one does not contain. In other words, they are the same if one can be mapped to the other by rearranging its rows. It is easy to see that for  $N_c = 1$  and  $N_c = 2$ , we obtain the optimal computation sequence. There exists only a single computation schedule matrix, so all sequences can be explored. For  $N_c = 3$ , there exist two unique computation schedule matrices which do not share a single row. With the initial prioritization selected by retaining priorities, we can transition from one computation schedule matrix to another between time steps as long as they share an identical row, i.e., an identical computation sequence. Consequently, retaining the result for an initial prioritization for  $N_c = 3$  restricts us to examining only three out of six possible computation sequences. More formally, we can construct a computation schedule graph  $\mathcal{G}_c = (\mathcal{V}_c, \mathcal{E}_c)$  with the set of all unique computation schedule matrices as vertices  $\mathcal{V}_c$ , which are connected by an edge if they share an identical row

$$(i - j) \in \mathcal{E}_c \iff \exists n, m: \mathbf{s}_n^{(i)} = \mathbf{s}_m^{(j)} \quad (18)$$

with the row  $\mathbf{s}_n^{(i)}$  belonging to the computation schedule matrix in vertex  $i$ , and the row  $\mathbf{s}_m^{(j)}$  belonging to the computation schedule matrix in vertex  $j$ .

**Theorem 4.** *Let the initial prioritization be selected by retaining priorities, and let the computation schedule matrix be created with Algorithm 2. For  $N_c \geq 4$ , we can explore all possible computation sequences of length  $N_c$  given enough time.*

*Proof.* We can prove this theorem by showing the computation schedule graph  $\mathcal{G}_c$  contains a spanning tree. Let an ascending sequence denote a sequence in which the indices of the agent

classes are consecutive for consecutive elements, except for the index  $N_c$ , which is followed by 1. We prove our theorem by showing that all computation schedule matrices are connected to a computation schedule matrix which contains the ascending sequence  $(\mathcal{V}_1, \dots, \mathcal{V}_{N_c})$ . All matrices containing the computation sequence  $(\mathcal{V}_1, \dots, \mathcal{V}_{N_c})$  are connected according to (18). All  $N_c$  different ascending sequences fit into one computation schedule matrix by shifting the starting index by one for each row. It follows that if any ascending sequence is part of a computation schedule matrix, the computation sequence  $(\mathcal{V}_1, \dots, \mathcal{V}_{N_c})$  is part of a connected matrix. If the initial sequence does not allow any ascending sequence to be part of the computation schedule matrix, exactly one element of this initial sequence is responsible for making exactly one of the ascending sequences invalid. Put differently: As long as there are two agent classes with consecutive indices in the initial sequence – both of which belong to a single ascending sequence and thus invalidate the same ascending sequence – one ascending sequence must be valid in the corresponding computation schedule matrix. In the case the initial sequence does not allow any ascending sequence to be part of the computation schedule matrix, we can place any ascending sequence and switch the element that would make the sequence invalid with its following element. This results in a sequence where  $N_c - 2$  elements are consecutive in their agent class index. If  $N_c \geq 4$ , more than two elements of this computation sequence are consecutive in their agent class index. As pointed out above, this matrix is connected to a matrix which contains a valid ascending sequence, which in turn is connected to a matrix containing the sequence  $(\mathcal{V}_1, \dots, \mathcal{V}_{N_c})$ . Therefore, a spanning tree of  $\mathcal{G}_c$  is rooted in the corresponding vertex.  $\square$

### 3.4 Discussion of our Approach for Simultaneous Computation

There are up to  $N_A!$  possible prioritizations  $N_{\text{prio}}$ , so the number of possible prioritizations exhibits factorial growth with the number of agents. The number of prioritizations which our approach considers equals the number of agent classes, which is upper bounded by the number of agents. Consequently, the ratio of explored prioritizations to all prioritizations decreases rapidly with the number of agents. However, the number of possible prioritizations is actually related to the connectivity of the coupling graph, which can be estimated by the vertex degree.

**Definition 10** (Degree). The degree

$$d^{(i)} = |\mathcal{V}^{(i)}| \quad (19)$$

of a vertex  $i$  denotes the number of its adjacent vertices. The number of incoming edges called in-degree is denoted by

$$d^{(i\leftarrow)} = |\mathcal{V}^{(i\leftarrow)}|. \quad (20)$$

The number of outgoing edges called out-degree is denoted by

$$d^{(i\rightarrow)} = |\mathcal{V}^{(i\rightarrow)}|. \quad (21)$$

**Theorem 5.** *The number of possible prioritizations  $N_{\text{prio}}$  of an undirected coupling graph  $\mathcal{G} = (\mathcal{V}, \mathcal{E})$  is upper bounded by*

$$N_{\text{prio}} \leq \left( \frac{2 \cdot |\mathcal{E}|}{N_A} \right)^{N_A} \leq \prod_{i \in \mathcal{V}} (d^{(i)} + 1). \quad (22)$$



*Proof.* The number of possible prioritizations is equal to the number of acyclic orientations of  $\mathcal{G}$ . The upper bound above is the upper bound on the number of acyclic orientations given in (Manber & Tompa, 1981, Theorem 10).  $\square$

*Remark 1.* According to Theorem 5, the number of possible prioritizations decreases with the sparsity of the coupling graph. Consequently, if we achieve a sparse coupling graph, the ratio of explored prioritizations to all prioritizations can be higher than the worst-case approximation of  $N_{\text{prio}}$  with  $N_A!$  suggests.

Our approach only explores a fraction of all possible prioritizations. However, if the networked planning problem changes only slightly from one time step to another, or if the approach is applied repeatedly, it can improve the solution quality incrementally. A significant benefit of our approach is that it is general and does not require any domain-specific knowledge.

## 4 Motion Planning for CAVs

MAMP is a variant of MAPF. The evaluation of the approach presented in this paper takes place in the context of MAMP for CAVs. We have the following correspondences between traditional MAPF and our formulation of MAMP for CAVs.

1. *System dynamics:* In MAPF, the dynamics of robots are usually abstracted in the graph search problem (e.g., Banfi, Shree, & Campbell, 2020; Li, Tinka, et al., 2021). In our MAMP, we explicitly consider the system dynamics in the planning problem by encoding motion in a motion primitive automaton (MPA).
2. *Objective:* In MAPF, the objective of agents is to plan a path to reach a target vertex in the graph representing the environment without collisions. In our MAMP, the objective of agents is to plan motions to stay close to a reference path without collisions. The reference path is the result of a routing layer and does not consider obstacles.
3. *Planning time horizon:* In MAPF, the planning time horizon is variable and extends until the agent has reached its target vertex. An agent plans once, and the plan reaches from the agent’s start vertex to its target vertex. In our MAMP, the planning time horizon is fixed. This allows for short and predictable computation times. An agent plans at every time step, thereby shifting its planning horizon, an approach known as receding horizon control (RHC).
4. *Environment representation:* In MAPF, the environment with its obstacles is encoded in a graph, where vertices represent locations at which agents can stop, and edges represent discretized motions of agents. In our MAMP, the environment with its obstacles is represented by a list of polygons. Each agent is required to avoid these polygons when planning motions.

There are works that go beyond traditional MAPF and extend the above-listed categorization; e.g., system dynamics are considered in (Alonso-Mora, Beardsley, & Siegwart, 2018; Le & Plaku, 2018; Luo, Chakraborty, & Sycara, 2016).

We formulate motion planning as an optimal control problem (OCP) in Section 4.1. We present our model for considering kinodynamic constraints in Section 4.2, and we show how we couple agents in Section 4.3. Section 4.4 presents our algorithm to solve the planning problem of each agent, which is based on model predictive control (MPC).

## 4.1 Motion Planning as an Optimal Control Problem

This section presents the ordinary differential equations describing the vehicle dynamics and our cost function before both are incorporated into an OCP for motion planning. The variables and equations in this section belong to a single agent  $i$ .

We refer to the entirety of all agents as an NCS. We control multiple agents in an NCS with a combination of prioritized planning and distributed model predictive control (DMPC) Richards and How (2007). This combination will be referred to as prioritized distributed model predictive control (Kloock, Scheffe, Botz, et al., 2019; Scheffe et al., 2022; Scheffe, Pedrosa, Flaßkamp, & Alrifaae, 2024; Scheffe, Xu, & Alrifaae, 2024). Finding the agents' control inputs is modeled as an OCP. We denote by agent OCPs the OCPs solved by the agents, and by networked OCP the OCP for the entire prioritized NCS.

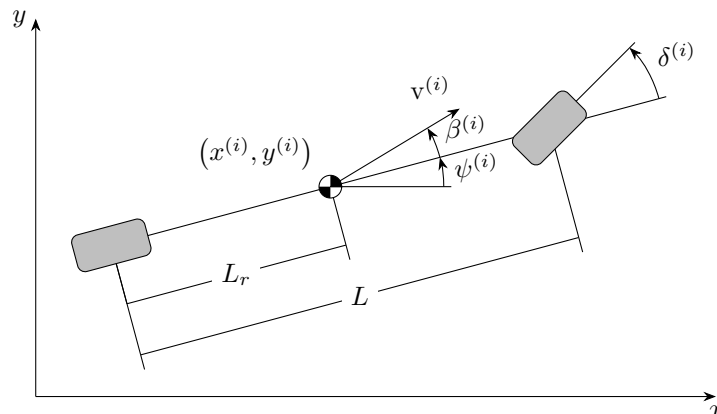


Figure 7: Kinematic single-track model of a vehicle. Figure redrawn from (Scheffe, Pedrosa, et al., 2023).

Figure 7 shows an overview of variables for the nonlinear kinematic single-track model (Rajamani, 2006, p. 21). Assuming low velocities, we model no slip on the front and rear wheels, and no forces acting on the vehicle. The resulting equations are

$$\begin{cases} \dot{x}^{(i)}(t) = v^{(i)}(t) \cdot \cos(\psi^{(i)}(t) + \beta^{(i)}(t)), \\ \dot{y}^{(i)}(t) = v^{(i)}(t) \cdot \sin(\psi^{(i)}(t) + \beta^{(i)}(t)), \\ \dot{\psi}^{(i)}(t) = v^{(i)}(t) \cdot \frac{1}{L} \cdot \tan(\delta^{(i)}(t)) \cos(\beta^{(i)}(t)), \\ \dot{v}^{(i)}(t) = u_v^{(i)}(t), \\ \dot{\delta}^{(i)}(t) = u_\delta^{(i)}(t), \end{cases} \quad (23)$$

with

$$\beta^{(i)}(t) = \tan^{-1} \left( \frac{L_r}{L} \tan(\delta^{(i)}(t)) \right), \quad (24)$$

where  $x^{(i)} \in \mathbb{R}$  and  $y^{(i)} \in \mathbb{R}$  describe the position of the center of gravity (CG),  $\psi^{(i)} \in [0, 2\pi)$  is the orientation,  $\beta^{(i)} \in [-\pi, \pi)$  is the side slip angle,  $\delta^{(i)} \in [-\pi, \pi)$  and  $u_\delta \in \mathbb{R}$  are the steering angle and its derivative respectively,  $v^{(i)} \in \mathbb{R}$  and  $u_v \in \mathbb{R}$  are the speed and acceleration of the CG respectively,  $L$  is the wheelbase length and  $L_r$  is the length from the rear axle to the CG.

The system dynamics defined in (23) are compactly written as

$$\dot{\mathbf{x}}^{(i)}(t) := \frac{d}{dt} \mathbf{x}^{(i)}(t) = f(\mathbf{x}^{(i)}(t), \mathbf{u}^{(i)}(t)) \quad (25)$$

with the state vector

$$\mathbf{x}^{(i)} = \begin{pmatrix} x^{(i)} & y^{(i)} & \psi^{(i)} & v^{(i)} & \delta^{(i)} \end{pmatrix}^T \in \mathbb{R}^5, \quad (26)$$

the control input

$$\mathbf{u}^{(i)} = \begin{pmatrix} u_v^{(i)} & u_\delta^{(i)} \end{pmatrix}^T \in \mathbb{R}^2 \quad (27)$$

and the vector field  $f$  defined by (23). Transferring (25) to a discrete-time nonlinear system representation yields

$$\mathbf{x}_{k+1}^{(i)} = f_d(\mathbf{x}_k^{(i)}, \mathbf{u}_k^{(i)}) \quad (28)$$

with a time step  $k \in \mathbb{N}$ , the vector field  $f_d: \mathbb{R}^5 \times \mathbb{R}^2 \rightarrow \mathbb{R}^5$ .

We define the cost function for agent  $i$  to minimize given a prioritization  $p$  in our motion planning problem as

$$J_p^{(i)}(k) = \sum_{l=1}^{N_p} \left( \mathbf{x}_{k+l|k}^{(i)} - \mathbf{r}_{k+l|k}^{(i)} \right)^T \mathbf{Q} \left( \mathbf{x}_{k+l|k}^{(i)} - \mathbf{r}_{k+l|k}^{(i)} \right) \quad (29)$$

with the prediction horizon  $N_p \in \mathbb{N}$ , a reference trajectory  $\mathbf{r}_{\cdot|k}^{(i)} \in \mathbb{R}^5$ , and the positive semi-definite, block diagonal matrix

$$\mathbf{Q} = \begin{pmatrix} \mathbf{I}_2 & \mathbf{0}_{2 \times 3} \\ \mathbf{0}_{3 \times 2} & \mathbf{0}_3 \end{pmatrix} \in \mathbb{R}^{5 \times 5}. \quad (30)$$

The OCP of agent  $i$  follows in (31). Since multiple agents are involved in the equation, we will include the agent superscript. We assume a full measurement or estimate of the state  $\mathbf{x}^{(i)}(k)$  is available at the current time  $k$ .

$$\begin{aligned} & \underset{\mathbf{u}_{\cdot|k}^{(i)}}{\text{minimize}} && J_p^{(i)}(k) \end{aligned} \tag{31a}$$

subject to

$$\mathbf{x}_{k+l+1|k}^{(i)} = f_d(\mathbf{x}_{k+l|k}^{(i)}, \mathbf{u}_{k+l|k}^{(i)}), \quad l = 0, \dots, N_p - 1, \tag{31b}$$

$$\mathbf{x}_{k+l|k}^{(i)} \in \mathcal{X}, \quad l = 1, \dots, N_p - 1, \tag{31c}$$

$$\mathbf{x}_{k+N_p|k}^{(i)} \in \mathcal{X}_f, \tag{31d}$$

$$\mathbf{x}_{k|k}^{(i)} = \mathbf{x}^{(i)}(k), \tag{31e}$$

$$\mathbf{u}_{k+l|k}^{(i)} \in \mathcal{U}, \quad l = 0, \dots, N_u - 1, \tag{31f}$$

$$c_c^{(i \leftarrow j)} \left( \mathbf{x}_{k+l|k}^{(i)}, \mathbf{x}_{k+l|k}^{(j)} \right) \leq 0, \quad l = 1, \dots, N_p, \quad j \in \mathcal{V}_p^{(i \leftarrow)}(k). \tag{31g}$$

Here,  $f_d: \mathbb{R}^n \times \mathbb{R}^m \rightarrow \mathbb{R}^n$  is a vector field resembling the discrete-time nonlinear system model with  $n \in \mathbb{N}$  as the number of states and  $m \in \mathbb{N}$  as the number of inputs,  $\mathbf{u}_{\cdot|k}^{(i)} = (\mathbf{u}_{k|k}^{(i)}, \mathbf{u}_{k+1|k}^{(i)}, \dots, \mathbf{u}_{k+N_u-1|k}^{(i)})$  is the input trajectory,  $\mathcal{X}$  is the set of feasible states,  $\mathcal{X}_f$  is the set of feasible terminal states, and  $\mathcal{U}$  is the set of feasible inputs. The coupling constraint  $c_c^{(i \leftarrow j)}: \mathbb{R}^n \times \mathbb{R}^n \rightarrow \mathbb{R}$  in (31g) enforces networked constraints among agents. The set of predecessors  $\mathcal{V}_p^{(i \leftarrow)}(k)$  contains the neighbors of  $i$  with higher priority given the prioritization  $p$ . An agent  $i$  solves its OCP after having received the predictions of all predecessors  $\mathcal{V}_p^{(i \leftarrow)}(k)$ . Afterwards, it communicates its own prediction to agents in  $\mathcal{V}_p^{(i \rightarrow)}(k)$ . Since the planning problem requires the predecessors' predictions in (31g), the agents must solve their OCPs in a sequential order. Each agent solves the OCP (31) repeatedly after a time step duration  $T_s$  and with updated values for the states and constraints, which establishes the RHC. Only the first input  $\mathbf{u}_{k|k}^{(i)}$  of the input trajectory is applied.

## 4.2 System Modeling with a Motion Primitive Automaton

This section presents how we model the state-continuous system (28) as an MPA (Frazzoli, Dahleh, & Feron, 2005; Scheffe, Pedrosa, et al., 2023). The MPA incorporates the constraints on system dynamics (31b), on control inputs (31f), and on both the steering angle and the speed (31c) and (31d).

From the system dynamics (23), we derive a finite state automaton which we call MPA and define as follows.

**Definition 11** (Motion primitive automaton, from (Scheffe, Pedrosa, et al., 2023)). An MPA is a 5-tuple  $(\mathcal{Q}, \mathcal{S}, \gamma, Q_0, \mathcal{Q}_f)$  composed of:

- $\mathcal{Q}$  is a finite set of automaton states  $Q$ ;
- $\mathcal{S}$  is a finite set of transitions  $S$ , also called motion primitives (MPs);
- $\gamma: \mathcal{Q} \times \mathcal{S} \times \mathbb{N} \rightarrow \mathcal{Q}$  is the update function defining the transition from one automaton state to another, dependent on the time step in the horizon;

- $Q_0 \in \mathcal{Q}$  is the initial automaton state;
- $Q_f \subseteq \mathcal{Q}$  is the set of final automaton states.

An automaton state is characterized by a specific speed  $v$  and steering angle  $\delta$ . An MP is characterized by an input trajectory and a corresponding state trajectory which starts and ends with the speed and steering angle of an automaton state. It has a fixed duration which we choose to be equal to the time step duration  $T_s$ . MPs can be concatenated to form longer state trajectories by rotation and translation. Our MPA discretizes both the state space with the update function  $\gamma$  and the time space with a fixed duration  $T_s$  for all MPs. This MPA replaces the system representation (28). Note that the dynamics model on which our MPA is based is interchangeable. Its complexity is irrelevant computation-wise for motion planning since MPs are computed offline. The MPA design forces vehicles to come to a complete stop at the end of the prediction horizon, which guarantees that solutions to (31) are recursively feasible; for details see our previous work (Scheffe et al., 2022; Scheffe, Pedrosa, et al., 2023).

### 4.3 Coupling of Vehicles

Although coupling all vehicles guarantees that coupling constraints for all vehicles will be considered, it also prolongs computation time and increases the number of prioritizations compared to coupling fewer vehicles. Therefore, we only couple vehicles that can potentially collide within the horizon  $N_p$ . We couple two vehicles at a time step  $k$  if at least one of their reachable sets intersects within the horizon  $N_p$ .

**Definition 12** (Reachable set of a time interval, from Scheffe, Xu, and Alrifae (2024)). The reachable set  $\mathcal{R}_{[t_1, t_2] | t_0}^{(i)}$  of the states of vehicle  $i$  between time  $t_1$  and time  $t_2$  starting from time  $t_0$  is

$$\mathcal{R}_{[t_1, t_2] | t_0}^{(i)} = \left\{ \bigcup_{t' \in [t_1, t_2]} \int_{t_0}^{t'} f(\mathbf{x}^{(i)}, \mathbf{u}^{(i)}) dt \mid \mathbf{x}^{(i)}(t_0) \in \mathcal{X}(t_0), \mathbf{u}^{(i)} \in \mathcal{U} \right\}.$$

The reachable sets  $\mathcal{R}_{[k+l, k+l+1] | k}^{(i)}$  over the prediction horizon of a vehicle can be computed offline with the MPA presented in Section 4.2. The set of coupling edges is

$$\mathcal{E}(k) = \left\{ (i - j) \mid i, j \in \mathcal{V}, i \neq j, \exists l \in \{0, \dots, N_p - 1\}; \mathcal{R}_{[k+l, k+l+1] | k}^{(i)} \cap \mathcal{R}_{[k+l, k+l+1] | k}^{(j)} \neq \emptyset \right\}, \quad (32)$$

This results in a time-variant coupling graph  $\mathcal{G}(k) = (\mathcal{V}, \mathcal{E}(k))$ .

### 4.4 Planning using Monte-Carlo Tree Search in a Model Predictive Control Framework

It is computationally hard to find the global optimum to the planning problem (31) due to its nonlinearity and nonconvexity. We substitute the system model (31b) with an MPA based on our previous work (Scheffe, Pedrosa, et al., 2023). Our MPA is general instead of tailored towards a specific environment. Therefore, our motion planning is a receding horizon tree search rather than a graph search. Obstacles are included in the state constraints (31c) of

our OCP formulation. In the Monte Carlo tree search (MCTS), we represent obstacles and predecessors’ trajectories as polygons.

The cost of edges in the tree is given by the cost function (31a). In this article, we use a sampling-based approach based on MCTS to find a path in the tree with low cost. Due to its anytime property, MCTS is a popular approach to complex control problems (Baby & HomChaudhuri, 2023; Choudhury, Gupta, Morales, & Kochenderfer, 2022; Kurzer, Zhou, & Marius Zöllner, 2018), as it allows balancing computation effort and solution quality. In each time step, our MCTS randomly expands a fixed number of vertices in the search tree. The algorithm thus inspects only a part of the complete search tree. After the expansions, the path in the search tree with the lowest cost according to (31a) is selected. The algorithm has no guarantee on optimality, but nearly constant computation time.

Because the MAMP runs online, vehicles require an input at every time step. However, since PP is incomplete (Theorem 1), the MCTS might fail to find a feasible solution. In such cases, vehicles reuse their previous, recursively feasible solution, ensuring safe motion plans (Scheffe et al., 2022).

## 5 Evaluation

We evaluate the presented approach for increasing solution quality by exploring multiple prioritizations in the context of multi-agent motion planning for CAVs. In Section 5.1, we describe the experiment setup, a scenario on a road network with up to 20 vehicles. In Sections 5.2 and 5.3, we evaluate the quality of the trajectories of the vehicles in the NCS, and the computation time of the NCS, respectively. In Section 5.4, we demonstrate our approach in an experiment in the CPM Lab, an open-source, remotely-accessible testbed for CAVs (Kloock et al., 2021). In Section 5.5, we discuss the implications of our results.

We compare our prioritization algorithm with five algorithms from the literature. Each algorithm is represented by a prioritization function  $p: \mathcal{V} \rightarrow \mathbb{N}$ . The first function prioritizes vehicles according to their vertex number (Alrifaae et al., 2016) and is denoted by  $p_{\text{constant}}$ . The second function prioritizes vehicles randomly at each time step (Bennewitz et al., 2002) and is denoted by  $p_{\text{random}}$ . The third function prioritizes vehicles with a constraint-based heuristic (Scheffe et al., 2022). A higher number of potential collisions with other vehicles results in a higher priority. The function is denoted by  $p_{\text{constraint}}$ . The fourth function prioritizes vehicles to decrease the number of agent classes, and thus the computation time, via graph coloring (Kuwata et al., 2007; Scheffe, Kahle, & Alrifaae, 2023). The function is denoted by  $p_{\text{color}}$ . The fifth function evaluates all possible prioritizations by solving the networked OCP for all acyclic orientations of the coupling graph. The function then chooses the prioritization which results in the lowest networked cost. It is denoted by  $p^*$ .

### 5.1 Setup

In our experiments, vehicles move on the road network shown in Figure 11. It consists of an urban intersection with eight incoming lanes, a highway, and highway on- and off-ramps. With this variety of road segments, we challenge our motion planner with merging, crossing, and overtaking scenarios.

Our MCTS uses the MPA illustrated in Figure 8, which is based on the kinematic single-track model as presented in (Scheffe, Pedrosa, et al., 2023). The MPA is discretized with

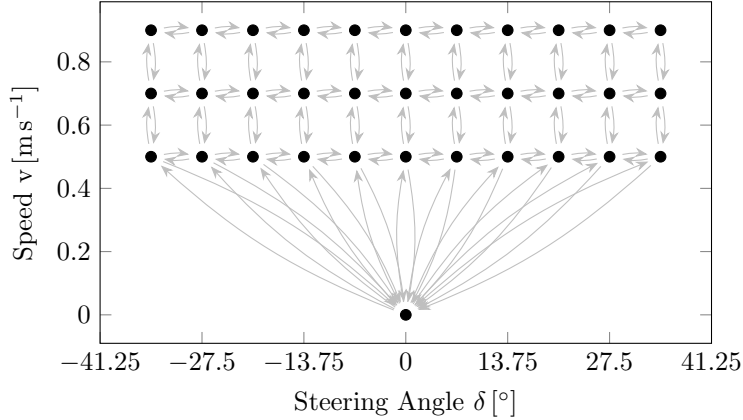


Figure 8: The MPA used in our experiments.

four speed levels.

We set the duration for our numerical experiments to 7 s with a time step size of 0.2 s. The vehicles start at random positions on the road network and follow a randomly selected path which starts and ends at the same point. The reference speeds for the vehicles in the experiments are selected as one of the speed levels of our MPA shown in Figure 8 at random.

During the experiment, the vehicles need to stay within the road boundaries according to the selected reference path. Lower-prioritized vehicles must avoid collisions with higher-prioritized ones. Therefore, coupling constraints with higher-prioritized vehicles reduce the set of feasible system states  $\mathcal{X}$  by the system states the higher-prioritized vehicles occupy during a motion primitive in the MPA (Scheffe, Pedrosa, et al., 2023). Two vehicles in an NCS are coupled whenever their reachable sets (Scheffe, Xu, & Alrifae, 2024) overlap. Therefore, the coupling graph is time-variant throughout an experiment.

Our algorithms ran on up to 20 Intel NUCs (NUC7i5BNK) connected via Ethernet, one for each participating vehicle. Each NUC was equipped with an Intel Core i5 7260U CPU with 2.2 GHz and 16 GB of RAM. The communication between two individual vehicles is realized by the ROS 2 Toolbox in MATLAB. The open-source algorithms are implemented in MATLAB<sup>1</sup>.

## 5.2 Solution Quality

We measure the solution quality with the networked cost  $J_p$  of a prioritization  $p$ . The networked cost according to the cost of the planning problem of each vehicle is given as

$$J_p = \sum_{k=0}^{k_{\text{experiment}}} \sum_{i=1}^{N_A} J_p^{(i)}(k), \quad (33)$$

with  $k_{\text{experiment}}$  being the number of time steps in the experiment, and  $J_p^{(i)}(k)$  given in (31a). Figure 9 shows the cost normalized to that of the prioritization  $p_{\text{constant}}$ .

<sup>1</sup>[github.com/embedded-software-laboratory/p-dmpc](https://github.com/embedded-software-laboratory/p-dmpc)

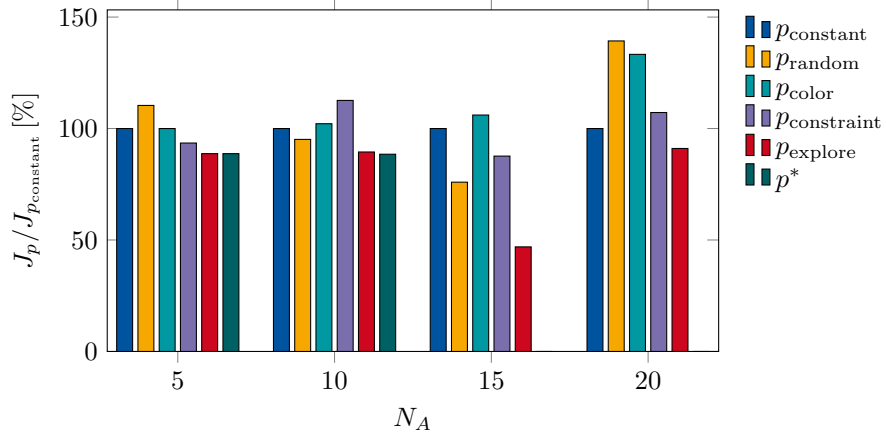


Figure 9: Comparison of the networked cost among multiple prioritization algorithms, normalized to the cost of  $p_{\text{constant}}$ . There is no value for  $p^*$  for 15 and 20 vehicles as the optimization did not terminate.

Our approach, denoted by  $p_{\text{explore}}$ , outperforms the approaches from the literature in terms of networked cost across all our experiments. For five and ten vehicles, the networked cost of our approach is within 1% of the cost of the optimal prioritization. For 15 vehicles, we reduce the networked cost by more than 53% compared to the baseline prioritization ( $p_{\text{constant}}$ ). There is no value for the cost of the optimal prioritization for 15 and 20 vehicles as the algorithm did not terminate in reasonable computation time.

### 5.3 Computation Time

With the following definitions, we formalize the computation time of the NCS based on our previous work (Scheffe, Kahle, & Alrifaaee, 2023). Let the sources of  $\vec{\mathcal{G}}$  be the set of vertices without incoming edges

$$\mathcal{V}_s = \{i \in \mathcal{V} \mid d^{(i \leftarrow)} = 0\} \quad (34)$$

and the sinks be the set of vertices without outgoing edges

$$\mathcal{V}_t = \{i \in \mathcal{V} \mid d^{(i \rightarrow)} = 0\}. \quad (35)$$

Note that since the coupling graph is a DAG, there is at least one source and one sink. Note further that the number of agent classes  $N_c$  is the diameter of  $\vec{\mathcal{G}}$  plus one. The diameter of a graph is the greatest length of any shortest path between each pair of vertices  $\mathcal{V} \times \mathcal{V}$ .

**Definition 13** (Path). A path in a graph  $\mathcal{G}$  is a sequence of edges connecting distinct vertices

$$(e_z)_{z=1}^n((i_1 \rightarrow i_2), (i_2 \rightarrow i_3), \dots, (i_n \rightarrow i_{n+1})), \quad (36)$$

with the domain  $\mathbb{N}$  and the codomain  $\mathcal{E}$ . The length of the path is defined as the number of edges  $n$ .



In the analysis of the computation time, we assume that the communication time is constant and negligible in comparison to the computation time for the planning problem. This assumption is justifiable since we use a wired connection between agents and compute a nonconvex planning problem. Then, the computation time  $T$  of the NCS is mainly determined by the time to solve the agent OCPs. To determine the computation time of the NCS, we add a virtual source  $S$  and a virtual sink  $G$  to the set of vertices  $\mathcal{V}$  of  $\vec{\mathcal{G}}$ , resulting in the set of vertices  $\mathcal{V}'$ . We furthermore add edges from the source  $S$  to all vertices in  $\mathcal{V}_s$ , and from all vertices in  $\mathcal{V}_t$  to the sink  $G$ , resulting in the set of edges  $\vec{\mathcal{E}}'$ . To obtain the computation time  $T$ , we weigh edges by a weighting function  $f_w: \mathcal{V}' \times \mathcal{V}' \rightarrow \mathbb{R}$

$$f_w((i \rightarrow j)) = \begin{cases} T^{(i)}, & \text{if } i \in \mathcal{V}, \\ 0, & \text{otherwise,} \end{cases} \quad (37)$$

with the computation time  $T^{(i)}$  of an edge’s respective starting vertex. The result is the computation graph  $\vec{\mathcal{G}}' = (\mathcal{V}', \mathcal{E}', f_w)$ . Figure 13 illustrates a computation graph. Let  $P_{\max} \subseteq \mathcal{V}' \times \mathcal{V}'$  denote the longest path between  $S$  and  $G$  in  $\vec{\mathcal{G}}'$ . The weight of this path corresponds to the computation time of the NCS

$$T = \sum_{(i \rightarrow j) \in P_{\max}} f_w((i \rightarrow j)). \quad (38)$$

For five and ten vehicles, the maximum computation time of our approach is two and 15 times faster than the optimal prioritization, respectively, while achieving a similar networked cost. For a larger number of vehicles, planning with optimal prioritization is computationally too expensive, as the number of possible prioritizations exhibits factorial growth in the number of vehicles. As shown in Figure 10, our approach scales well with the number of vehicles and only slightly increases the computation time compared to the baseline prioritization. In particular, the median computation time is only slightly increased. We discuss the larger increase in maximum computation time in Section 5.5.

## 5.4 Experiment

We conducted an experiment with ten vehicles in the CPM Lab (Kloock et al., 2021). A snapshot of the experiment is shown in Figure 11, a video of the experiment is available online<sup>2</sup>. In order to achieve real-time capability, we combine our approach with our previous work of limiting the number of agent classes (Scheffe, Xu, & Alrifaae, 2024). We chose a limit of  $N_c = 2$ .

In our experiment, we achieve a networked computation time with a median of 72 ms and a maximum of 111 ms across all time steps. With our time step duration of  $T_s = 200$  ms, this networked computation time allows enough leeway for other subordinate computations and for communication.

## 5.5 Discussion

Experiments have shown that constant priorities can outperform time-varying priorities even in dynamic environments (Scheffe et al., 2022). A possible explanation is that agents

---

<sup>2</sup>[youtu.be/Mb59zQ3j3s0](https://youtu.be/Mb59zQ3j3s0)

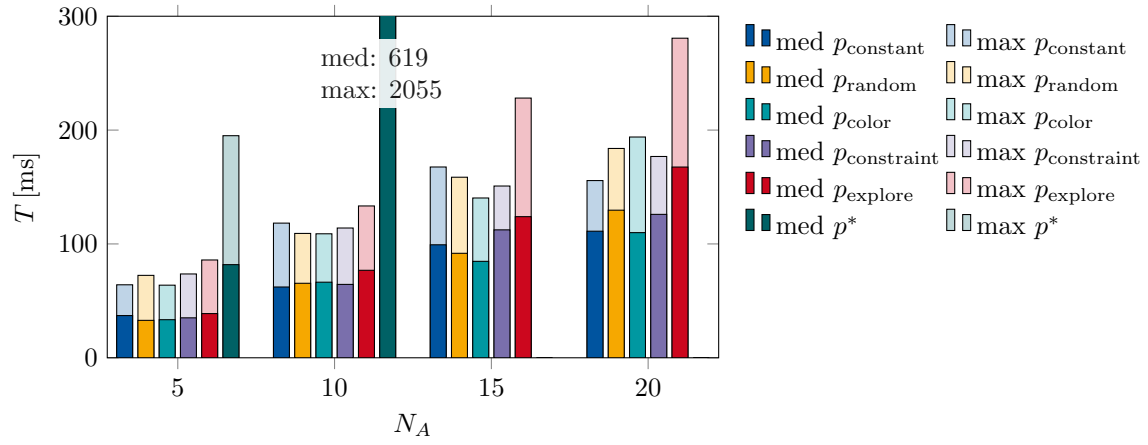


Figure 10: Comparison of the networked computation time among multiple prioritization algorithms. There is no value for  $p^*$  for 15 and 20 vehicles as the optimization did not terminate.

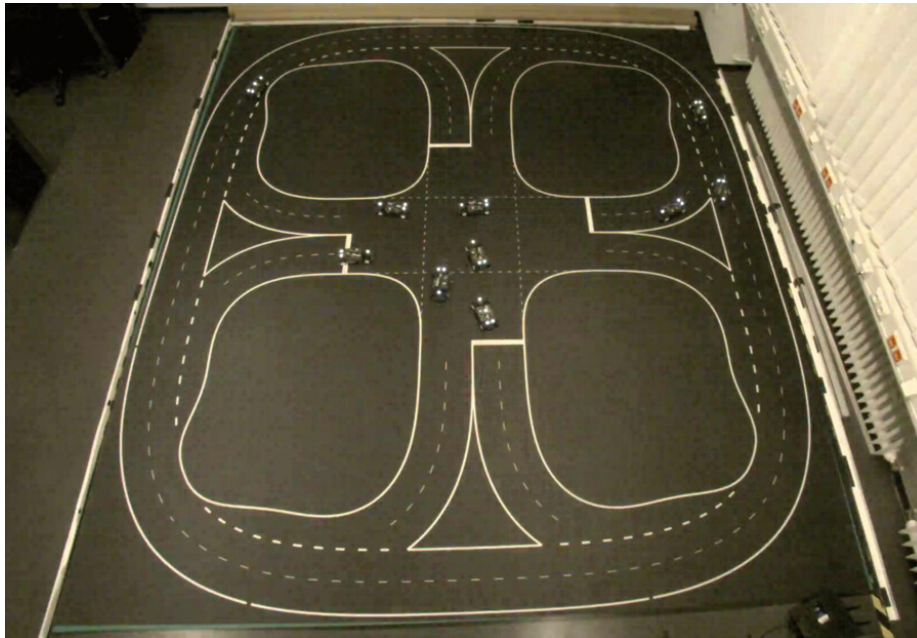


Figure 11: Experiment in the CPM Lab with ten vehicles.

can make full use of the predictive capabilities of MPC, as the agent OCPs remain similar between time steps. However, there are instances in which a different prioritization yields better solutions or a different prioritization is required to even enable progress at all. In contrast to approaches from the literature, our approach can both remain at a prioritization or switch to another one, determined by the networked cost.

As the networked computation time is equal to the longest path in the computation graph  $\bar{\mathcal{G}}'$ , the increase in computation time is more noticeable for a larger number of vehicles. When the vehicle number is larger, the number of agent classes increases, as shown in Figure 12. Our approach explores one prioritization per agent class. When exploring

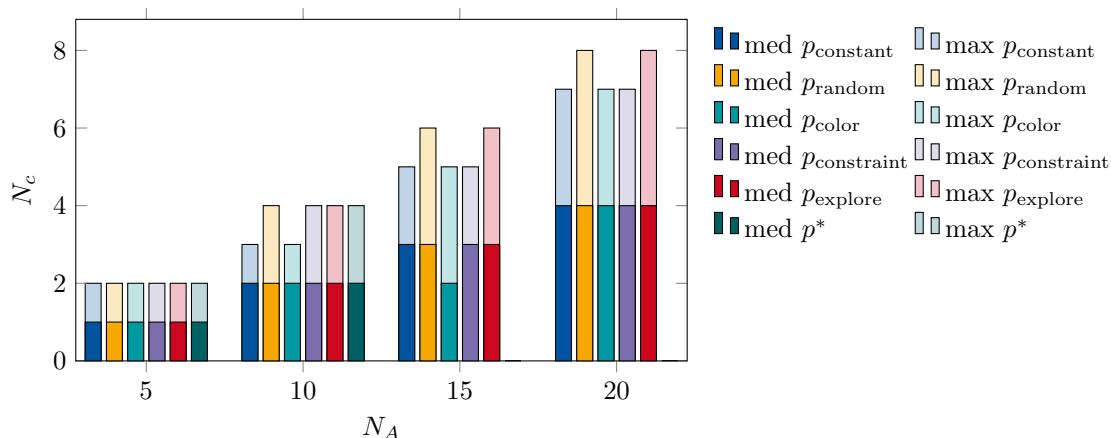


Figure 12: Comparison of the number of agent classes among multiple prioritization algorithms. The value of  $p^*$  corresponds to the number of agent classes of the selected prioritization. There is no value for  $p^*$  for 15 and 20 vehicles as the optimization did not terminate.

multiple prioritizations, the networked computation time is at least as high as the maximum of all considered prioritizations. It can even be higher, as computations of multiple prioritizations are interdependent: agents need to finish their computations before the next prioritization can be computed. This concept is visualized in Figure 13 for four agents in a coupling graph with three levels and thus three prioritizations. Figure 13a displays an example computation schedule matrix, which contains the agent classes in the computation sequence of Figure 5. Figure 13b displays the corresponding computation graph. A vertex corresponds to the computation of a planning problem. Each agent appears three times since we compute three prioritizations simultaneously. The edges in black indicate the couplings of agents in the three distinct prioritizations. Since an agent can only compute one solution at a time, the subgraphs of these prioritizations are connected by additional edges in teal accounting for the sequential computation. If we weigh all outgoing edges with the computation time associated with solving the vertex' planning problem, the networked computation time is determined by the longest path in the computation graph. Through both the increased number of computations and the higher connectivity of these computations in the computation graph, there is a greater possibility to obtain a larger computation time compared to other prioritization approaches. This effect is especially noticeable when the computation time of the agents is dissimilar.

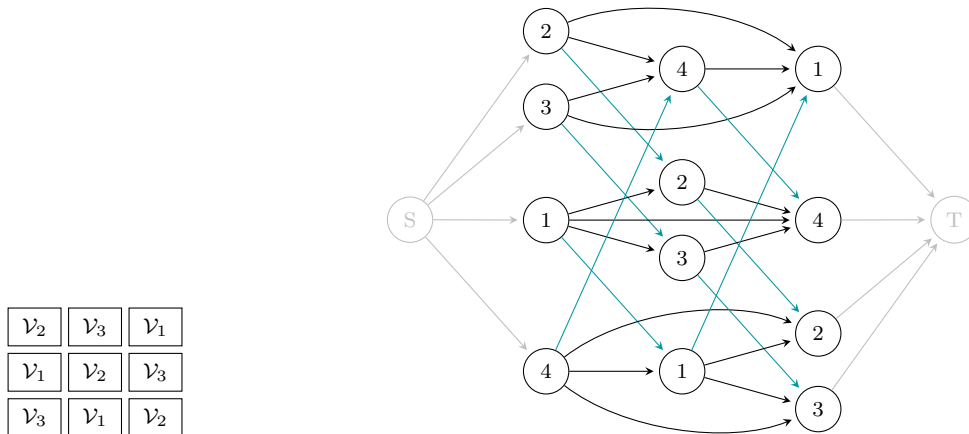


Figure 13: Example computation schedule matrix and computation graph for our explorative prioritization. Four agents in three agent classes simultaneously compute three different prioritizations. Agent classes are from the example in Figure 5.

*Remark 2.* If the computation time of all agents for each planning problem of every prioritization is exactly equal, there is no overhead in computation time for our approach. In practice, exactly equal computation times are difficult to achieve.

In our approach, the number of prioritizations explored is equal to the number of agent classes. For each prioritization, communication is required. Consequently, this results in an increase in the communication effort by a factor of the number of agent classes. Additionally, agents communicate the cost of their solution so that our algorithm can determine the networked cost of each prioritization. In practice, the exchanged data is small, as it only consists of the trajectory over the prediction horizon and the cost of the planning problem. However, if communication resources are scarce, this property needs to be accounted for.

## 6 Conclusion

We presented an approach to utilize idle time in prioritized planning to simultaneously compute with multiple prioritizations. With our approach, we can achieve high solution quality with significantly less computational effort than that of sequential computation of the considered prioritizations. Additionally, our approach is general, as it does not rely on domain-specific heuristics.

Our approach can simultaneously examine as many prioritizations as there are agent classes. The higher the number of agent classes, the more prioritizations are examined. However, the number of possible prioritizations increases more quickly with the number of

agent classes. Therefore, our approach is more likely to find the optimal prioritization with a lower number of agent classes. Additionally, a lower number of agent classes results in a smaller increase in computation time. These benefits make the approach well-suited to be combined with limiting the number of agent classes for real-time computation (Scheffe, Xu, & Alrifaae, 2024).

We claim that our approach is general and can thus be transferred to prioritized computations in other applications. It needs to be analyzed how well the approach transfers, especially regarding the communication effort and the computation time. Since the planning problems of multiple prioritizations are solved simultaneously, the communication effort compared to computing with a single prioritization is multiplied by the number of agent classes. In our experiments, agents communicated via LAN. It seems likely that the communication effort is decreased if computations run on the same machine, and increased if agents communicate via WLAN. In any case, the gain in solution quality must outweigh the increase in communication effort compared to computing with a single prioritization. We presented solving an OCP as a control method to find control inputs and to generate a prediction. However, our approach works well with any control method in which agents have similar computation times. Therefore, the approach could also be evaluated with different control methods. We presented simulations with up to 20 agents and eight agent classes, and an experiment with ten agents and two agent classes. Conducting experiments with a larger number of agents and agent classes would be interesting to study the convergence to the optimal prioritization. An application with a convex OCP might be suitable to still achieve real-time capable computations. In this paper, our algorithm selects the prioritizations randomly. The algorithm might improve if it instead selects prioritizations based on knowledge from the solution quality of prioritizations it has solved before.

## 7 Acknowledgements

This research was funded by the Deutsche Forschungsgemeinschaft (DFG, German Research Foundation) within the Priority Program SPP 1835 “Cooperative Interacting Automobiles” (grant number: KO 1430/17-1).

## References

- Almhanna, M. S., Al-Turaihi, F. S., & Murshedi, T. A. (2023, October). Reducing waiting and idle time for a group of jobs in the grid computing. *Bulletin of Electrical Engineering and Informatics*, *12*(5), 3115–3123. doi: 10.11591/eei.v12i5.4729
- Alonso-Mora, J., Beardsley, P., & Siegwart, R. (2018, April). Cooperative Collision Avoidance for Nonholonomic Robots. *IEEE Transactions on Robotics*, *34*(2), 404–420. doi: 10.1109/TRO.2018.2793890
- Alrifaae, B., Hefeler, F.-J., & Abel, D. (2016). Coordinated Non-Cooperative Distributed Model Predictive Control for Decoupled Systems Using Graphs. *IFAC-PapersOnLine*, *49*(22), 216–221. doi: 10.1016/j.ifacol.2016.10.399
- Azarm, K., & Schmidt, G. (1997, April). Conflict-free motion of multiple mobile robots based on decentralized motion planning and negotiation. In *Proceedings of International*

- Conference on Robotics and Automation* (Vol. 4, p. 3526-3533 vol.4). doi: 10.1109/ROBOT.1997.606881
- Baby, T. V., & HomChaudhuri, B. (2023, May). Monte Carlo Tree Search Based Trajectory Generation for Automated Vehicles in Interactive Traffic Environments. In *2023 American Control Conference (ACC)* (pp. 4431–4436). doi: 10.23919/ACC55779.2023.10156530
- Banfi, J., Shree, V., & Campbell, M. (2020, September). Planning High-Level Paths in Hostile, Dynamic, and Uncertain Environments. *Journal of Artificial Intelligence Research*, *69*, 297–342. doi: 10.1613/jair.1.12077
- Barer, M., Sharon, G., Stern, R., & Felner, A. (2021, September). Suboptimal Variants of the Conflict-Based Search Algorithm for the Multi-Agent Pathfinding Problem. *Proceedings of the International Symposium on Combinatorial Search*, *5*(1), 19–27. doi: 10.1609/socs.v5i1.18315
- Bennewitz, M., Burgard, W., & Thrun, S. (2002, November). Finding and optimizing solvable priority schemes for decoupled path planning techniques for teams of mobile robots. *Robotics and Autonomous Systems*, *41*(2), 89–99. doi: 10.1016/S0921-8890(02)00256-7
- Çam, Ö. N., & Sezen, H. K. (2020, March). The formulation of a linear programming model for the vehicle routing problem in order to minimize idle time. *Decision Making: Applications in Management and Engineering*, *3*(1), 22–29. doi: 10.31181/dmame2003132h
- Čáp, M., Novák, P., Kleiner, A., & Selecký, M. (2015, July). Prioritized Planning Algorithms for Trajectory Coordination of Multiple Mobile Robots. *IEEE Transactions on Automation Science and Engineering*, *12*(3), 835–849. doi: 10.1109/TASE.2015.2445780
- Chalaki, B., & Malikopoulos, A. A. (2022). A Priority-Aware Replanning and Resequencing Framework for Coordination of Connected and Automated Vehicles. *IEEE Control Systems Letters*, *6*, 1772–1777. doi: 10.1109/LCSYS.2021.3133416
- Chen, D., Hajidavalloo, M. R., Li, Z., Chen, K., Wang, Y., Jiang, L., & Wang, Y. (2023, November). Deep Multi-Agent Reinforcement Learning for Highway On-Ramp Merging in Mixed Traffic. *IEEE Transactions on Intelligent Transportation Systems*, *24*(11), 11623–11638. doi: 10.1109/TITS.2023.3285442
- Choudhury, S., Gupta, J. K., Morales, P., & Kochenderfer, M. J. (2022, March). Scalable Online Planning for Multi-Agent MDPs. *Journal of Artificial Intelligence Research*, *73*, 821–846. doi: 10.1613/jair.1.13261
- Erdmann, M., & Lozano-Pérez, T. (1987, November). On multiple moving objects. *Algorithmica*, *2*(1), 477. doi: 10.1007/BF01840371
- Frazzoli, E., Dahleh, M., & Feron, E. (2005, December). Maneuver-based motion planning for nonlinear systems with symmetries. *IEEE Transactions on Robotics*, *21*(6), 1077–1091. doi: 10.1109/TRO.2005.852260
- Guo, T., & Yu, J. (2024, October). Expected 1.x Makespan-Optimal Multi-Agent Path Finding on Grid Graphs in Low Polynomial Time. *Journal of Artificial Intelligence Research*, *81*, 443–479. doi: 10.1613/jair.1.16299
- Kloock, M., Scheffe, P., Botz, L., Maczijewski, J., Alrifaae, B., & Kowalewski, S. (2019). Networked Model Predictive Vehicle Race Control. In *IEEE Intell. Transp. Syst. Conf. ITSC* (pp. 1552–1557). doi: 10.1109/ITSC.2019.8917222
- Kloock, M., Scheffe, P., Maczijewski, J., Kampmann, A., Mokhtarian, A., Kowalewski, S.,

- & Alrifaae, B. (2021). Cyber-Physical Mobility Lab: An Open-Source Platform for Networked and Autonomous Vehicles. In *Eur. Control Conf. ECC* (pp. 1937–1944). doi: 10.23919/ECC54610.2021.9654986
- Kloock, M., Scheffe, P., Marquardt, S., Maczijekowski, J., Alrifaae, B., & Kowalewski, S. (2019). Distributed Model Predictive Intersection Control of Multiple Vehicles. In *IEEE Intell. Transp. Syst. Conf. ITSC* (pp. 1735–1740). doi: 10.1109/ITSC.2019.8917117
- Korte, B., & Vygen, J. (2018). *Combinatorial Optimization: Theory and Algorithms* (Vol. 21). Berlin, Heidelberg: Springer Berlin Heidelberg. doi: 10.1007/978-3-662-56039-6
- Kurzer, K., Zhou, C., & Marius Zöllner, J. (2018, June). Decentralized Cooperative Planning for Automated Vehicles with Hierarchical Monte Carlo Tree Search. In *2018 IEEE Intelligent Vehicles Symposium (IV)* (pp. 529–536). doi: 10.1109/IVS.2018.8500712
- Kuwata, Y., Richards, A., Schouwenaars, T., & How, J. P. (2007, July). Distributed Robust Receding Horizon Control for Multivehicle Guidance. *IEEE Transactions on Control Systems Technology*, 15(4), 627–641. doi: 10.1109/TCST.2007.899152
- Le, D., & Plaku, E. (2018, October). Cooperative, Dynamics-based, and Abstraction-Guided Multi-robot Motion Planning. *Journal of Artificial Intelligence Research*, 63, 361–390. doi: 10.1613/jair.1.11244
- Li, J., Hoang, T. A., Lin, E., Vu, H. L., & Koenig, S. (2023, June). Intersection Coordination with Priority-Based Search for Autonomous Vehicles. *Proceedings of the AAAI Conference on Artificial Intelligence*, 37(10), 11578–11585. doi: 10.1609/aaai.v37i10.26368
- Li, J., Ruml, W., & Koenig, S. (2021, May). EECBS: A Bounded-Suboptimal Search for Multi-Agent Path Finding. *Proceedings of the AAAI Conference on Artificial Intelligence*, 35(14), 12353–12362. doi: 10.1609/aaai.v35i14.17466
- Li, J., Tinka, A., Kiesel, S., Durham, J. W., Kumar, T. K. S., & Koenig, S. (2021). Lifelong Multi-Agent Path Finding in Large-Scale Warehouses. *Proceedings of the AAAI Conference on Artificial Intelligence*, 35(13), 11272–11281.
- Luo, W., Chakraborty, N., & Sycara, K. (2016, July). Distributed dynamic priority assignment and motion planning for multiple mobile robots with kinodynamic constraints. In *2016 American Control Conference (ACC)* (pp. 148–154). Boston, MA, USA: IEEE. doi: 10.1109/ACC.2016.7524907
- Ma, H., Harabor, D., Stuckey, P. J., Li, J., & Koenig, S. (2019, July). Searching with Consistent Prioritization for Multi-Agent Path Finding. *Proceedings of the AAAI Conference on Artificial Intelligence*, 33, 7643–7650. doi: 10.1609/aaai.v33i01.33017643
- Ma, H., Li, J., Kumar, T. S., & Koenig, S. (2017, May). Lifelong Multi-Agent Path Finding for Online Pickup and Delivery Tasks. In *Proceedings of the 16th Conference on Autonomous Agents and MultiAgent Systems* (pp. 837–845). Richland, SC: International Foundation for Autonomous Agents and Multiagent Systems.
- Mak, H.-Y., Rong, Y., & Zhang, J. (2014, May). Sequencing Appointments for Service Systems Using Inventory Approximations. *Manufacturing & Service Operations Management*, 16(2), 251–262. doi: 10.1287/msom.2013.0470
- Manber, U., & Tompa, M. (1981, October). The effect of number of Hamiltonian paths on the complexity of a vertex-coloring problem. In *22nd Annual Symposium on Foundations of Computer Science (sfcs 1981)* (pp. 220–227). doi: 10.1109/SFCS.1981.47

- McKay, B. D., & Wanless, I. M. (2005, October). On the Number of Latin Squares. *Annals of Combinatorics*, 9(3), 335–344. doi: 10.1007/s00026-005-0261-7
- Pan, Z., Wang, R., Bi, Q., Zhang, X., & Yu, J. (2024, August). RH-ECBS: Enhanced conflict-based search for MRPP with region heuristics. *Robotica*, 1–11. doi: 10.1017/S0263574724000894
- Rajamani, R. (2006). *Vehicle Dynamics and Control*. New York: Springer Science.
- Richards, A., & How, J. P. (2007, September). Robust distributed model predictive control. *International Journal of Control*, 80(9), 1517–1531. doi: 10.1080/00207170701491070
- Scheffe, P., Dorndorf, G., & Alrifaae, B. (2022). Increasing Feasibility with Dynamic Priority Assignment in Distributed Trajectory Planning for Road Vehicles. In *IEEE Int. Conf. Intell. Transp. Syst. ITSC* (pp. 3873–3879). doi: 10.1109/ITSC55140.2022.9922028
- Scheffe, P., Kahle, J., & Alrifaae, B. (2023). *Reducing Computation Time with Priority Assignment in Distributed Control*. doi: 10.36227/techrxiv.20304015.v2
- Scheffe, P., Pedrosa, M. V. A., Flaßkamp, K., & Alrifaae, B. (2023). Receding Horizon Control Using Graph Search for Multi-Agent Trajectory Planning. *IEEE Trans. Control Syst. Technol.*, 31(3), 1092–1105. doi: 10.1109/TCST.2022.3214718
- Scheffe, P., Pedrosa, M. V. A., Flaßkamp, K., & Alrifaae, B. (2024). Prioritized Trajectory Planning for Networked Vehicles Using Motion Primitives. In C. Stiller, M. Althoff, C. Burger, B. Deml, L. Eckstein, & F. Flemisch (Eds.), *Cooperatively Interacting Vehicles: Methods and Effects of Automated Cooperation in Traffic* (pp. 253–275). Cham: Springer International Publishing. doi: 10.1007/978-3-031-60494-2\_9
- Scheffe, P., Xu, J., & Alrifaae, B. (2024). *Limiting Computation Levels in Prioritized Trajectory Planning with Safety Guarantees*. doi: 10.13140/RG.2.2.32731.03368
- Shahar, T., Shekhar, S., Atzmon, D., Saffidine, A., Juba, B., & Stern, R. (2021, March). Safe Multi-Agent Pathfinding with Time Uncertainty. *Journal of Artificial Intelligence Research*, 70, 923–954. doi: 10.1613/jair.1.12397
- Sharon, G., Stern, R., Felner, A., & Sturtevant, N. R. (2015, February). Conflict-based search for optimal multi-agent pathfinding. *Artificial Intelligence*, 219, 40–66. doi: 10.1016/j.artint.2014.11.006
- Silver, D. (2005). Cooperative Pathfinding. *Proceedings of the AAAI Conference on Artificial Intelligence and Interactive Digital Entertainment*, 1(1), 117–122. doi: 10.1609/aiide.v1i1.18726
- van den Berg, J., & Overmars, M. (2005, August). Prioritized motion planning for multiple robots. In *2005 IEEE/RSJ International Conference on Intelligent Robots and Systems* (pp. 430–435). doi: 10.1109/IROS.2005.1545306
- Wu, W., Bhattacharya, S., & Prorok, A. (2020, May). Multi-Robot Path Deconfliction through Prioritization by Path Prospects. In *2020 IEEE International Conference on Robotics and Automation (ICRA)* (pp. 9809–9815). Paris, France: IEEE. doi: 10.1109/ICRA40945.2020.9196813
- Yao, N., & Zhang, F. (2018, August). Resolving Contentions for Intelligent Traffic Intersections Using Optimal Priority Assignment and Model Predictive Control. In *2018 IEEE Conference on Control Technology and Applications (CCTA)* (pp. 632–637). Copenhagen: IEEE. doi: 10.1109/CCTA.2018.8511561
- Yu, J. (2016, January). Intractability of Optimal Multirobot Path Planning on Planar Graphs. *IEEE Robotics and Automation Letters*, 1(1), 33–40. doi: 10.1109/LRA.2015



.2503143

- Yu, J. (2020, March). Average case constant factor time and distance optimal multi-robot path planning in well-connected environments. *Autonomous Robots*, 44(3-4), 469–483. doi: 10.1007/s10514-019-09858-z
- Yu, J., & LaValle, S. (2013, June). Structure and Intractability of Optimal Multi-Robot Path Planning on Graphs. *Proceedings of the AAAI Conference on Artificial Intelligence*, 27(1), 1443–1449. doi: 10.1609/aaai.v27i1.8541
- Zhang, S., Li, J., Huang, T., & Koenig, S. (2022). Learning a Priority Ordering for Prioritized Planning in Multi-Agent Path Finding. *Proceedings of the Symposium on Combinatorial Search*, 15(1), 208–216.